Basal Cells Show Increased Expression of Aromatase and Estrogen Receptor α in Prostate Epithelial Lesions of Male Aging Rats

Mônica Morais-Santos,[1,2]* Hipácia Werneck-Gomes,[1]* Gabriel H. Campolina-Silva,[1] Leticia C. Santos,[1] Germán A. B. Mahecha,[1] Rex A. Hess,[3] and Cleida A. Oliveira[1]

[1]Department of Morphology, Universidade Federal de Minas Gerais, CEP 31270-901, Belo Horizonte, Minas Gerais, Brazil; [2]Department of Animal Biology, Universidade Federal de Viçosa, CEP 36570-900, Viçosa, Minas Gerais, Brazil; and [3]Department of Comparative Biosciences, University of Illinois, Urbana, Illinois 61802-6199

Besides androgens, estrogen signaling plays a key role in normal development and pathologies of the prostate. Irreversible synthesis of estrogens from androgens is catalyzed by aromatase. Interestingly, animals lacking aromatase do not develop cancer or prostatitis, whereas those with overexpression of aromatase and, consequently, high estrogen levels develop prostatitis and squamous metaplasia via estrogen receptor 1 (ERα). Even with this evidence, the aromatase expression in the prostate is controversial. Moreover, little is known about the occurrence of age-dependent variation of aromatase and its association with histopathological changes commonly found in advanced age, a knowledge gap that is addressed herein. For this purpose, the immunoexpression of aromatase was evaluated in the prostatic complex of young adult to senile Wistar rats. ERα was also investigated, to extend our understanding of estrogen responsiveness in the prostate. Moderate cytoplasmic immunoreactivity for aromatase was detected in the glandular epithelium. Eventually, some basal cells showed intense staining for aromatase. The expression pattern for aromatase appeared similar in the normal epithelium when young and senile rats were compared; this result was corroborated by Western blotting. Conversely, in senile rats, there was an increase in the frequency of basal cells intensely stained for aromatase, which appeared concentrated in areas of intraepithelial proliferation and prostatitis. These punctual areas also presented increased ERα positivity. Together, these findings suggest a plausible source for hormonal imbalance favoring estrogen production, which, by acting through ERα, may favor the development of prostatic lesions commonly found in advanced age. (***Endocrinology*** **159: 723–732, 2018)**

There is a significant and growing body of evidence that estrogen has a role in normal development of the prostate, through binding to specific nuclear estrogen receptors—estrogen receptor (ER) 1 (ERα) and 2 (ERβ) (1). Nevertheless, estrogens are also involved in the induction of premalignant and malignant lesions of the prostate (2–8). Irreversible synthesis of estrogens from androgens is catalyzed by aromatase, an enzyme encoded by the *CYP19* gene (9, 10). Interestingly, aromatase knockout mice do not develop cancer or inflammation of the prostate, whereas those with overexpression of aromatase develop prostatitis, as well as squamous metaplasia (4, 11, 12). Despite this evidence suggesting the involvement of aromatase and estrogens in prostate pathology, information about the expression of aromatase in this organ is still controversial for humans and rodents.

In human prostate, earlier studies detected aromatase activity in homogenates of normal and hyperplasic prostates (13, 14). Furthermore, aromatase protein and messenger RNA (mRNA) were detected in hyperplasic

ISSN Online 1945-7170

Received 21 August 2017. Accepted 1 November 2017.
First Published Online 7 November 2017

*These authors contributed equally to this study.

Abbreviations: Arom+basal cell, basal cell that stained intensely for aromatase; CK HMW, high-molecular-weight cytokeratin; ER, estrogen receptor; ERα, estrogen receptor 1; ERβ, estrogen receptor 2; mRNA, messenger RNA; PBS, phosphate-buffered saline; PIA, proliferative inflammatory atrophy; RRID, Research Resource Identifier; v/v, volume-to-volume ratio.

and malignant tissues, as well as in tumor cell lines (15–19). Conversely, others could not detect the expression of aromatase or its activity in prostate tissue and tumor cell lines (20–23). Distribution of aromatase within the epithelial and stromal compartments is also controversial, because some studies have found the protein and mRNA confined to stroma of hyperplasic and cancerous tissue (16, 24), whereas others detected expressions of aromatase in stroma and epithelium of normal and hyperplasic tissue (17, 18, 25). A more complete study, conducted by using several prostatic cell lines in addition to human prostate samples, did not detect aromatase by immunohistochemistry in benign tissue, but did detected it at the transcript and protein levels by polymerase chain reaction and Western blotting, respectively, in benign stroma, and in the tumor epithelium (26). Detection of aromatase activity and mRNA restricted to cancerous tissue has also been described by others (27).

Information about aromatase in the rodent prostate is even more scarce. Enzymatic activity in microsomes obtained from ventral prostate and Dunning R3327H rat adenocarcinoma were the first description (28). Aromatase mRNA was detected in mouse prostate but at variable levels and bordering on the limit of detectability (11). Aromatase protein and mRNA were also described in the prostate epithelium of control and bisphenol A-treated rats (29).

Serum and intraprostatic testosterone levels decline with advancing age, whereas estradiol levels are sustained or increased, thus changing the androgen-to-estrogen ratio, which has been implicated in the development of prostatic lesions (9). Recently, we reported that aging Wistar rats naturally develop histopathological alterations in the prostate epithelium, which were similar to those observed in humans, including proliferative, inflammatory, and premalignant lesions (30). These altered areas presented a focal reduction of ERβ expression, suggesting a potential disruption in estrogen signaling (30). Although aromatase, the key enzyme involved in estrogen synthesis, appears to be implicated in prostatic pathology commonly found in advanced age, little is known about age-dependent variation in prostate expression of aromatase. Therefore, the aging Wistar rat was used as a model for the study of aromatase in prostate pathology.

Material and Methods

Animals

The investigation was carried out using the prostatic complex from adult male Wistar rats aged 3, 6, 12, 18, and 24 months (n = 10 per age). The experimental procedures were approved by the local Ethical Committee in Animal Experimentation (process no. 286/2008 Comissão de Ética no Uso de Animais/Universidade Federal de Minas Gerais). The rats were housed in the animal facilities at the Universidade Federal de Minas Gerais, Brazil, under controlled conditions of light (12 hours of lights on, 12 hours of lights off) and temperature (22°C), with *ad libitum* access to food (Nuvital Nutrientes, Colombo, Brazil) and water.

Tissue preparation

After reaching the ages of interest, the rats were weighed and anesthetized with a mixture of 50 mg/kg sodium pentobarbital and 10 mg/kg ketamine hydrochloride (intraperitoneally). The tissues were rinsed with saline by transcardial perfusion via the left ventricle and then fixed by perfusion of 10% neutral buffered formalin. After fixation, the ventral, dorsal, and lateral prostate lobes were dissected, weighed, sectioned, and embedded in paraffin (Histosec Pastilles; Merck, Darmstadt, Germany) for hematoxylin and eosin staining and immunohistochemical and immunofluorescence assays (n = 5 per age). Otherwise, the animals were perfused only with saline solution (n = 5 per age) and the prostate lobes were immediately dissected, weighed, frozen in liquid nitrogen, and stored at −80°C until used for Western blotting assay.

Immunohistochemistry

Tissues sectioned at 5.0 μm were deparaffinized, rehydrated, blocked for endogenous peroxidase, and then submitted to a standard microwave method of antigen retrieval (31). Nonspecific bindings were blocked by immersion of the sections in 10% normal goat serum for 1 hour before incubation overnight at 4°C with the primary antibodies listed in Table 1. Negative control animals received only saline buffer in place of the primary antibodies. After washing, the sections were exposed for 1 hour at room temperature to a biotinylated goat anti-rabbit antibody [Research Resource Identifier (RRID): AB_2313609; catalog no. E0432; Dako, Carpinteria, CA] diluted 1:100 for aromatase detection or to a biotinylated goat anti-mouse antibody (RRID: AB_2687905; catalog no. E0433; Dako) diluted 1:100 for ERα, high-molecular-weight cytokeratin (CK HMW), and MCM7 detection. The sections were then incubated with the avidin-biotin complex (Vectastain Elite ABC Kit; Vector Laboratories, Burlingame, CA) for 30 minutes. Immunoreactions were visualized by immersion in 0.05% (weight-to-volume ratio) 3,3′ diaminobenzidine solution containing 0.01% [volume-to-volume ratio (v/v)] hydrogen peroxide in 0.05 M Tris-HCl buffer (pH 7.6), followed by Mayer's hematoxylin counterstaining.

Validation of the antiaromatase antibody was performed using testis and ovary as positive controls (1, 32–34) and skeletal muscle tissue as negative controls (32), which were processed in parallel to prostatic tissues (Fig. 1F).

Quantitative analysis

Aromatase immunostaining intensity in basal and luminal cells was determined after the evaluation of six random images per section at ×400 magnification, obtained using the Pannoramic Viewer software (3DHISTECH; Budapest, Hungary). All images were modified to grayscale and inverted using Adobe Photoshop CS6 (Adobe Systems, San Jose, CA). Then, cytoplasm of the basal cells was traced digitally and the mean intensity of pixels was measured by using ImageJ software

Table 1. Primary Antibodies Used in This Study

Peptide/Protein Target	Antigen Sequence (if Known)	Name of Antibody	Manufacturer, Catalog No.	Species Raised in; Monoclonal or Polyclonal	Dilution Used	RRID
Aromatase		Antiaromatase	Sigma-Aldrich, A7981	Rabbit; polyclonal	1:3000 (IHC); 1:1000 (IF and WB)	AB_1845043
β-actin		Anti–β-actin, AC-74	Sigma-Aldrich, A5316	Mouse; monoclonal	1:5000 (WB)	AB_476743
Estrogen receptor α		Anti–estrogen receptor α, ER-7G5	Zymed	Mouse; monoclonal	1:500 (IHC); 1:100 (IF)	AB_2335714
High-molecular-weight cytokeratin		Anti–CK HMW, 34βE12	Dako, M0630	Mouse; monoclonal	1:250 (IHC); 1:25 (IF)	AB_2687834
MCM7		CDC47/MCM7 Ab-2	Neomarkers, MS-862-P0	Mouse; monoclonal	1:500 (IHC)	AB_145298
Ki67		Anti-Ki67 antibody	Abcam, ab15580	Rabbit; polyclonal	1:300 (IF)	AB_443209

Abbreviations: IF, immunofluorescence; IHC, immunohistochemistry; WB, Western blotting.

(National Institutes of Health, Bethesda, MD). The same procedure was performed on four subsequent luminal cells. Background intensity was determined by tracing a blank area adjacent to the measured cells, which then was subtracted from the intensity obtained for the stained cytoplasm, providing a final pixel intensity. Basal epithelial cells were identified as the small cells in contact with the basement membrane and presenting visible nuclei (35). Most basal cells also had cytoplasmic projections toward the lumen.

In addition, the number of basal cells intensely stained for aromatase was determined in the normal epithelium and also in areas presenting lesions typically found in each aging prostate lobe, as described previously (30). The lesions included the following: atrophic epithelium in the ventral prostate, hyperplastic epithelium in the dorsal prostate, and epithelium with proliferative inflammatory atrophy (PIA) in the lateral prostate. The quantification of basal cells was performed in epithelial areas of 20 luminal cells randomly selected in the lesion areas. Twenty cells were also counted in the normal epithelium, adjacent to lesions. The results were expressed as percentage of basal cells intensely stained for aromatase per luminal cells. In addition, the presence of lesions in the rat prostate at different ages was scored after histological examination. The values were expressed as percentages: incidence of lesions to incidence of Arom+basal cells in these lesions.

The number of basal cells intensely stained for aromatase was also evaluated according to the adjacent stromal inflammation. For this purpose, a score of 1 to 3 for each inflammatory foci was designed based on the number of stromal inflammatory cells counted per foci, as follows: score 1, $<$20 cells; score 2, 21 to 50 cells; score 3, $>$50 cells. The number of basal epithelial cells presenting intense aromatase positivity was evaluated according to the traced score.

Immunofluorescence

To confirm the identity of the basal cells, aromatase was colocalized in the ventral, dorsal, and lateral prostate lobes with the CK HMWs, a basal cell marker (36). The sections and antigenic recovery were performed as described for immunohistochemistry. The tissue sections were then permeabilized in phosphate-buffered saline (PBS) containing triton X-100 0.5% (v/v) and incubated at room temperature for 90 minutes with 5% normal goat serum and PBS/ bovine serum albumin 1% to block nonspecific bindings. After this step, the sections were incubated overnight at 4°C with mix solution containing the primary antibodies antiaromatase and anti-CK HMW, listed in Table 1. After washing in PBS, the sections were incubated for 90 minutes at room temperature with a solution containing the secondary antibodies goat anti-mouse CF555 conjugated (RRID: AB_2336060; catalog no. SAB4600066; Sigma-Aldrich, Dorset, UK), diluted 1:100, and goat anti-rabbit fluorescein isothiocyanate conjugated (RRID: AB_259384; catalog no. F0382; Sigma-Aldrich), diluted 1:200 in PBS/ bovine serum albumin 1%. Negative controls received only saline buffer in place of the primary antibodies. The 4′,6-diamidino-2-phenylindole dihydrochloride staining (RRID: AB_2629482; catalog no. D1306; Thermo Fisher Scientific, Waltham, MA) was used to identify the cell nucleus. Finally, the fluorescence signals were obtained using a C2 Eclipse Ti confocal microscope (Nikon, Nogoya, Japan) equipped with specific filters for detection of fluorescein isothiocyanate (green), CF555 (red), and 4′,6-diamidino-2-phenylindole (blue).

To correlate the profile of cell proliferation and the ERα expression, immunofluorescence was also performed, as described, aiming to colocalize ERα and proliferation marker Ki67 (Table 1).

Toluidine blue staining

Acidified toluidine blue staining was performed to highlight metachromatic mast cells (11). For this, tissues sectioned at 3.0 μm were deparaffinized, rehydrated, and stained in 0.5% Toluidine Blue O (Sigma-Aldrich) and 1% sodium borate solution for 15 seconds. The sections were then washed in running water and, after drying, the slides were mounted.

Western blotting

Western blot assays were conducted in the prostate of Wistar rats to evaluate possible changes in aromatase protein levels during aging and also to confirm the specificity of the antibody used. For this purpose, total protein was extracted from frozen ventral and lateral prostates and measured as described previously (30). Because aromatase expression in the prostate is controversial, the protein content extracted from rat testes was also loaded in assays as a positive control. Previous work, using the same antibody, has demonstrated a single band of 55 kDa for aromatase in the rat testis (33). The proteins (40 μg/lane) were separated by 10% sodium dodecyl sulfate polyacrylamide

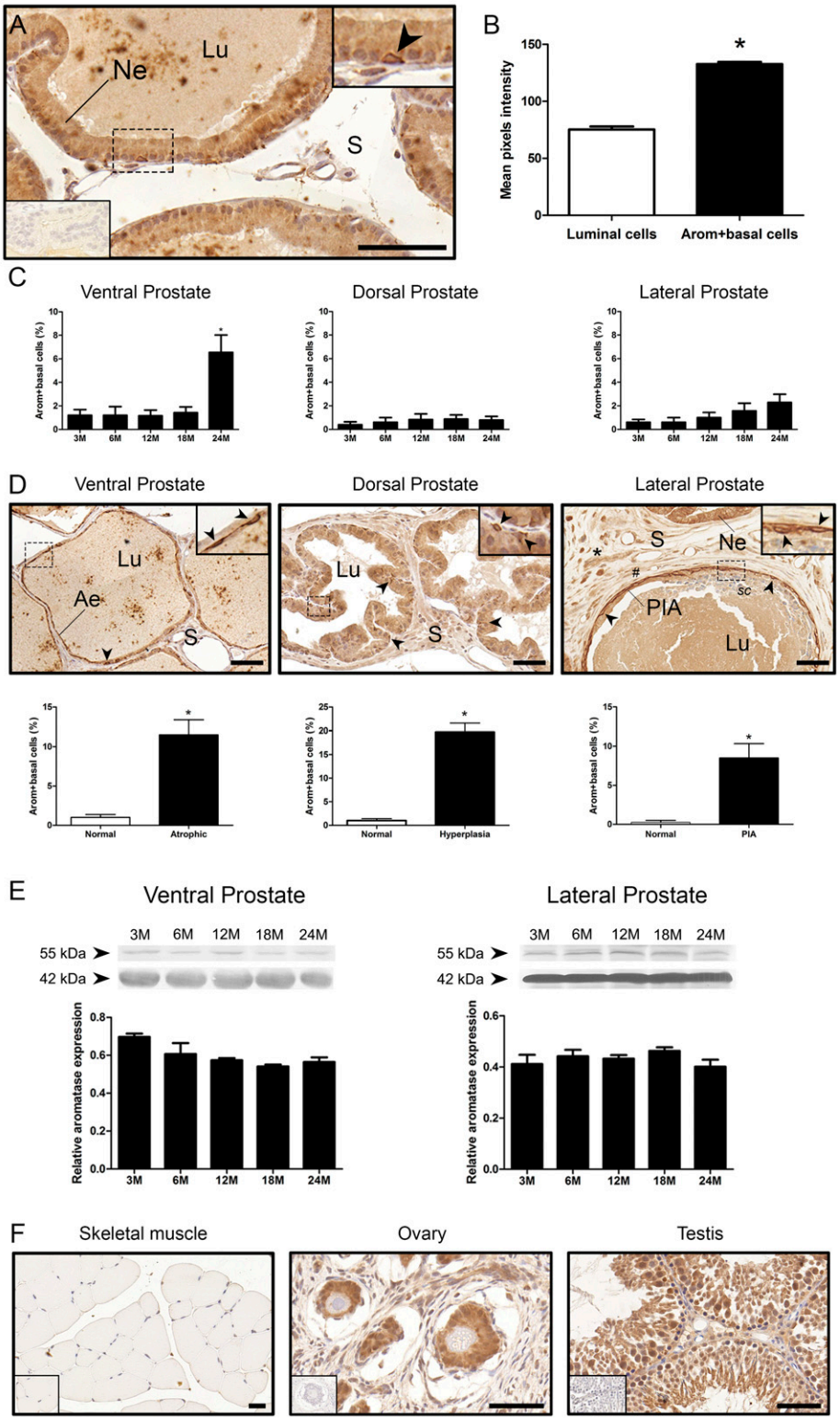

Figure 1. Expression of aromatase in the aging rat prostatic complex. (A) Aromatase immunoreactivity seen in the cytoplasm of epithelial cells of young rats, showing higher staining in basal cells (upper inset). Basal cells that stained intensely for aromatase (Arom+basal cells) are indicated by arrowheads. (B) Graphical representation comparing the staining intensity in Arom+basal cells and the adjacent luminal cells of the prostate epithelium (n = 5). (C) Frequency of Arom+basal cells in the ventral, dorsal, and lateral prostate with aging. (D) Immunostaining and graphical representation showing increased frequency of Arom+basal cells (arrowheads) in areas of atrophy in the ventral prostate, hyperplasia in the dorsal prostate, and PIA in the lateral prostate of aging rats. Inflammatory infiltration is indicated by the asterisk (*) in (D). (E) Western blotting of aromatase in rat ventral and lateral prostates at different ages. Representative bands from the assay (55 kDa for aromatase and 42 kDa for β-actin) and graphical representation of the densitometric analysis (n = 3 per group). (F) Validation of the aromatase antibody, using skeletal muscle as negative and ovary and testis as positive control tissues. Inferior insets show the negative control. Scale bars = 50 μm. *$P \leq 0.05$. #, thickening of the stroma; Ae, atrophic epithelium; Lu, lumen; Ne, normal epithelium; S, stroma; *sc*, sloughed cells into the lumen.

gel electrophoresis, transferred to a nitrocellulose membrane, and immersed for 1 hour in 10% normal goat serum to block nonspecific bindings. Then, we incubated the membrane overnight in a cold chamber containing the antiaromatase antibody listed in Table 1. After washing in PBS-Tween 0.05%, the membrane was exposed for 1 hour at room temperature to a biotinylated goat anti-rabbit antibody (RRID: AB_2313609; catalog no. E0432; Dako) diluted 1:1000 in PBS. Immunolabeling was visualized with a solution of 0.1% of 3,3′ diaminobenzidine in PBS containing 0.05% (weight-to-volume ratio) chloronaphthol, 16.6% (v/v) methanol, and 0.04% (v/v) H_2O_2. The procedure was performed in duplicate and repeated in three independent assays to confirm the results. The aromatase band intensity for each group was estimated using Image J software (National Institutes of Health) and normalized with the β-actin signal used as internal control.

Statistical analysis

The quantitative data were statistically analyzed with GraphPad Prism 5 software (GraphPad Software, La Jolla, CA). Initially, the Shapiro-Wilk test was used to check normality of the data sets. When normality was confirmed, the data were analyzed by Student *t* test to compare means between two groups or analysis of variance plus Tukey *post hoc* test to compare more than two groups. Otherwise, the Mann-Whitney test or Kruskal-Wallis plus Dunn *post hoc* test was used for comparisons between two or more groups, respectively. The results were expressed graphically as mean ± standard error of the mean. Spearman correlation was also used to evaluate the number of basal epithelial cells presenting intense aromatase positivity according to traced score for adjacent stromal inflammation. The significance level used for all tests was $P \leq 0.05$.

Results

Aromatase in the prostatic complex of aging rats

Moderate aromatase immunoreactivity was detected in the cytoplasm of epithelial cells (Fig. 1A). Interestingly, some cells with the location and morphology of basal epithelial cells eventually appeared more intensely stained for the enzyme compared with adjacent luminal cells (Fig. 1A), as confirmed by computer-assisted image analysis (Fig. 1B). These cells were found scattered along the normal epithelium and were small, triangular, and usually presenting cytoplasmic extensions projecting toward the lumen. Hereafter, the basal cells that stained intensely for aromatase are referred to in this article as Arom+ basal cells.

As the rats aged, the pattern of aromatase immunoreaction did not change in the normal epithelium. This finding was confirmed by Western blotting; pixel intensities of the aromatase bands were similar when ventral and lateral prostates of young adult and senile rats were compared (Fig. 1E). However, in specific areas of the aging prostate epithelium, which included proliferative and atrophic lesions, there was a reduction in cytoplasmic aromatase expression in the luminal cells (Fig. 2).

The number of Arom+basal cells did not change when the normal epithelium was considered, except for the ventral prostate, where an increased percentage of these cells was observed at age 24 months (Fig. 2C). Morphological changes were observed throughout aging in all prostatic lobes and the incidence of lesions increased as the animals aged (Table 2). A remarkable finding was that older rats (18 and 24 months of age) showed higher density of Arom+basal cells in areas containing tissue lesions (Table 2), which were typically found in small groups but were also seen forming an almost continuous layer in the base of the epithelium (Figs. 1 and 2). Some of these features were characteristic across each prostate lobe, but different in specific location (Fig. 1D). In the ventral prostate, there was an increase of about 10-fold in the frequency of Arom+basal cells in areas of epithelial atrophy, whereas in the dorsal prostate, there was a 20-fold increase in the frequency of these cells in areas of hyperplasia, compared with those of the adjacent normal epithelium (Fig. 1D). The lateral prostate presented the highest proportion of Arom+basal cells, especially in areas of PIA, in which the increase was > 30-fold compared with the adjacent normal epithelium (Fig. 1D). We also observed increased number of these cells in acini presenting metaplasia or cribriform intraepithelial proliferation (Fig. 2).

It should also be noted that the Arom+basal cells were also observed in areas associated with inflammatory foci, being more commonly found in the lateral prostate, a pattern confirmed by the strong positive correlation between the percentage of these cells and the stromal inflammation score ($r = 0.85$; $P < 0.0001$; Fig. 3). Metachromatic mast cells and polymorphonuclear cells were observed in the inflammatory foci (Fig. 3). It was common in these areas to observe the presence of sloughed cells in the lumen and a thicker peritubular stromal layer surrounding the adenomeres (Figs. 2 and 3).

The identity of the Arom+basal cells was confirmed by colocalization of aromatase and the basal cell marker CK HMW (Fig. 4). In line with immunohistochemistry, Arom+basal cells were found sporadically in the normal epithelium but at higher density in tissue lesions, as highlighted in areas of PIA and squamous metaplasia of the senile lateral prostate (Fig. 4). These cells were also found in areas of atrophic epithelium and an area of cribriform intraepithelial proliferation in the ventral lobe (Fig. 4), as well as in areas of hyperplasia in the dorsal prostate (data not shown).

ERα in the prostatic complex

The increase in aromatase expression was found in areas showing increases in epithelial proliferation (Fig. 2), areas described by others as having lower expressions of ERβ (30). Therefore, we decided to investigate whether the levels of ERα might also be changed with aging. In

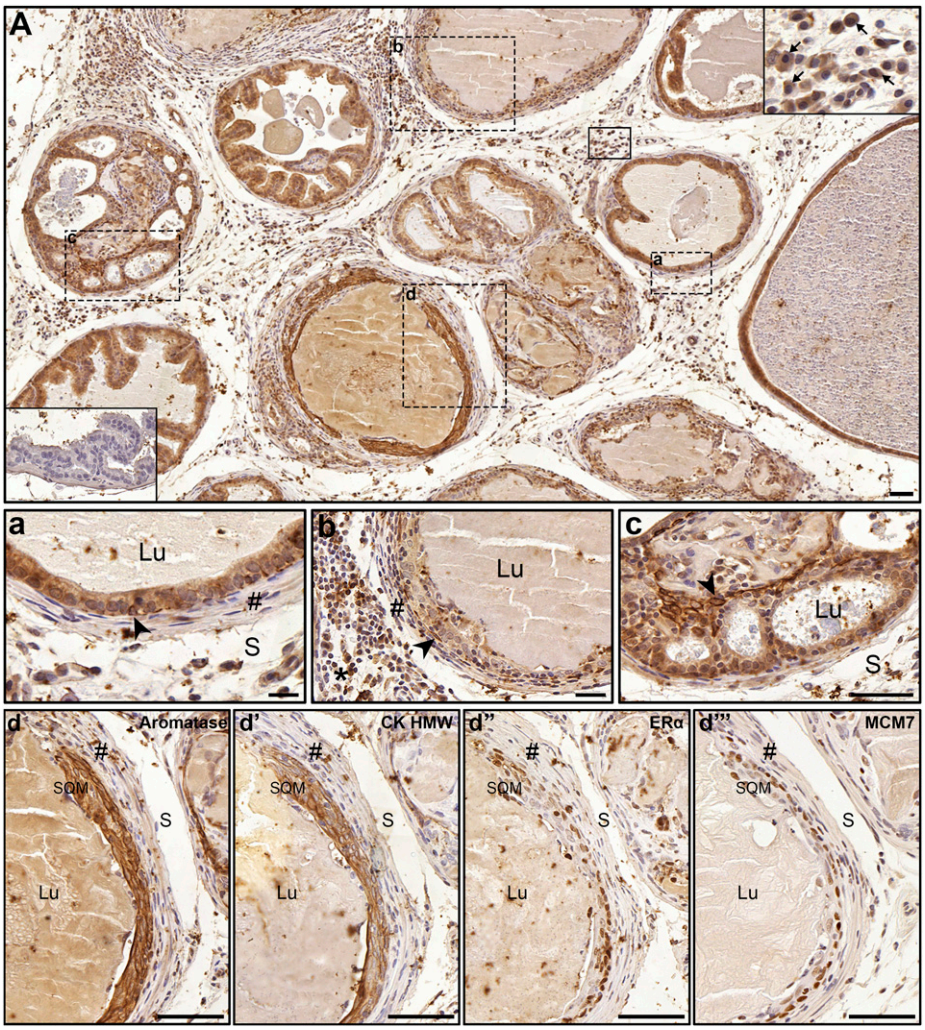

Figure 2. Changes in aromatase immunostaining in epithelial cells of the lateral prostate of senile rats. (A) Low-power magnification showing different epithelial lesions adjacent to intense inflammation in the stroma. (a–d) High-power magnification showing specific areas of (A). Inferior inset shows the negative control; superior inset shows inflammatory infiltrate (Arom+basal cells are indicated by arrowheads). (a) Moderate cytoplasmic expression in the epithelium without apparent morphological alteration. (b) Cytoplasmic reduction of aromatase in metaplastic epithelium. Inflammatory infiltration is indicated by the asterisk (*). (c) Cribriform intraepithelial proliferation showing groups of Arom+basal cells. (d) Squamous metaplasia showing intense aromatase immunostaining in basal cells, as confirmed by (d') serial section of the same lesion stained for CK HMW. (d'') Groups of ERα-positive nuclei located in the base of the epithelium were also observed in the same squamous metaplasia, suggestive of basal cell nuclei. (d''') MCM7 staining as marker of proliferation. Scale bars = 50 μm. #, thickening of the stroma; Lu, lumen; S, stroma; SQM, squamous metaplasia.

normal epithelium of the rat prostate, at all ages analyzed, some isolated nuclei were positive for ERα (Fig. 5). However, in focal areas showing increases in epithelial proliferation and increased presence of inflammatory cells, there was a consistent increase in ERα-positive cells. In the epithelium, ERα-positive cells were found in small groups, instead of being scattered across the epithelium (Fig. 5). The positive nuclei were mainly found in areas of intraepithelial proliferation (*i.e.*, ventral and dorsal prostates), hyperplasia (*i.e.*, dorsal prostate), and squamous metaplasia and PIA (*i.e.*, lateral prostate).

A frequent finding in the lateral prostate was the presence of groups of ERα-positive nuclei located in the base of the epithelium, suggestive of basal cell nuclei (Fig. 2C and Fig. 5). These cells were also found mainly in areas of intraepithelial proliferation associated with thickening of the adjacent stroma and inflammatory cells (Fig. 2C and Fig. 5).

Considering the putative proliferative activity of ERα and the higher rates of cell proliferation found in lesions areas of the aging prostates (37), we investigated whether the increased number of ERα-positive cells were proliferating cells. Colocalization of ERα and the proliferation marker Ki67 revealed that many of the proliferating cells found in lesions areas were also positive for ERα (Fig. 5).

Discussion

In this study, we investigated aromatase expression in the prostatic complex of young adult to senile Wistar rats.

Table 2. Incidence of Lesions in the Prostate of Rats According to Age

Lesion	Age				
	3 Months	6 Months	12 Months	18 Months	24 Months
Atrophy	0/0	5/0	25/25	60/66	80/100
Hyperplasia	0/0	19/0	25/33	67/50	83/66
Cribriform proliferation	0/0	0/0	0/0	0/0	17/50
Intraepithelial proliferation	0/0	5/0	25/0	47/0	54/0
Proliferative inflammatory atrophy	0/0	0/0	0/0	13/100	40/100
Squamous metaplasia	0/0	0/0	0/0	20/50	60/66

Values are expressed as incidence of lesions/incidence of Arom+ basal cells in these lesions.

Our data indicated that aromatase is widely expressed in the rat prostate epithelium. Interestingly, some basal epithelial cells showed a stronger staining intensity for the enzyme. In senile rats, there was an increase in the frequency and distribution of the Arom+basal cells in focal areas of intraepithelial proliferation, PIA, squamous metaplasia, and prostatitis. ERα-positive epithelial cells were also restricted to these same areas of proliferative and inflammatory alterations. These findings suggest a plausible local source of estrogen production, which, by acting through ERα, may lead to focal areas of pathological changes in the aging prostate. It is important to highlight that this direct association between the responsive estrogen system and the rat prostate lesions was obtained using a natural *in vivo* aging model without genetic, hormonal, or chemical induction.

Aromatase was found distributed primarily in epithelial cells, but was also found in the stromal compartment of rat prostate, even though the total tissue protein concentration observed by Western blot was low. These results corroborate previous data from mouse, rat, rhesus monkey, and man that described low amounts of aromatase activity, protein, or mRNA in the prostate (11, 18, 26, 28, 29, 38). The pattern of aromatase immunostaining appeared similar in areas of normal epithelium for all prostate lobes when young and senile rats were compared. Western blot analysis confirmed this finding, because similar bands for the enzyme were detected in the ventral and lateral prostates at all ages analyzed. Consistent with these results, intraprostatic estradiol concentrations were not changed with age, as previously found (30).

Sporadic Arom+basal cells were found in the normal prostate epithelium of young adult and senile rats.

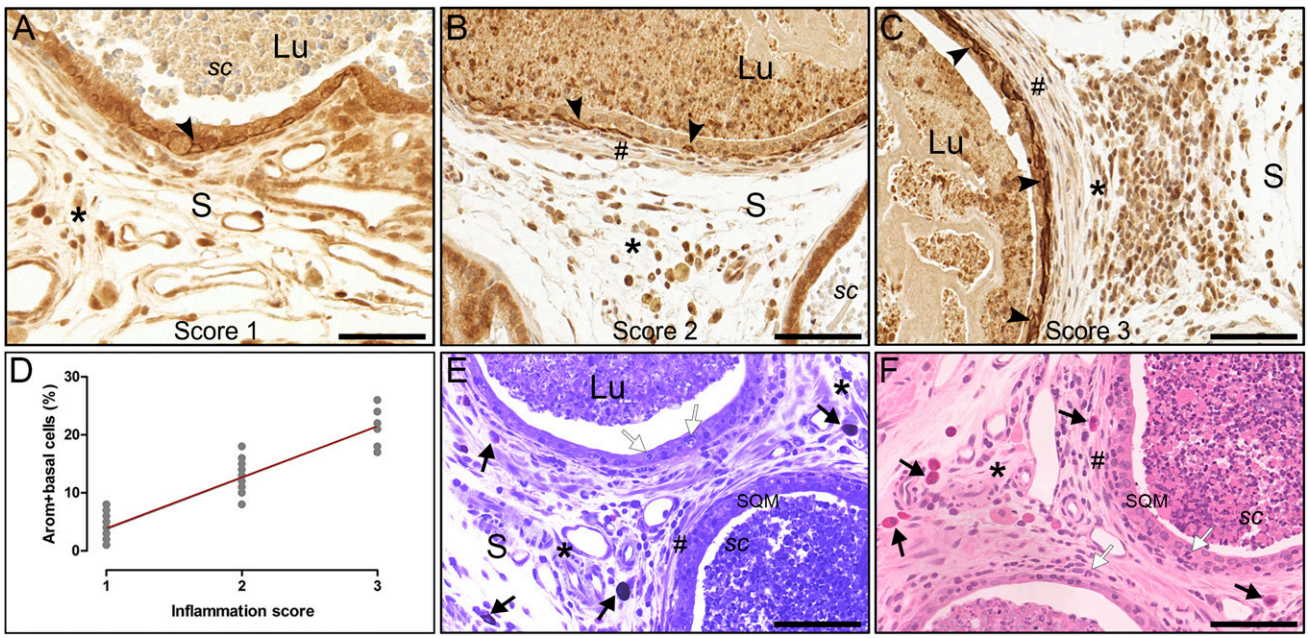

Figure 3. Arom+basal cells (arrowheads) in the epithelium associated with stromal inflammation in the lateral prostate of aging rats. (A–C) Representative pictures of the stromal inflammation traced for the score. (D) Strong positive correlation between the number of Arom+basal cells and the inflammation score ($r = 0.85$; $P < 0.0001$). (E) Toluidine blue staining. (F) Hematoxylin and eosin staining. (E, F) Mast cells are indicated by arrows; hollow arrows indicate polymorphonuclear cells. Scale bars = 50 μm. #, thickening of the stroma; *, inflammatory infiltrate; Lu, lumen; S, stroma; *sc*, sloughed cells into the lumen; SQM, squamous metaplasia.

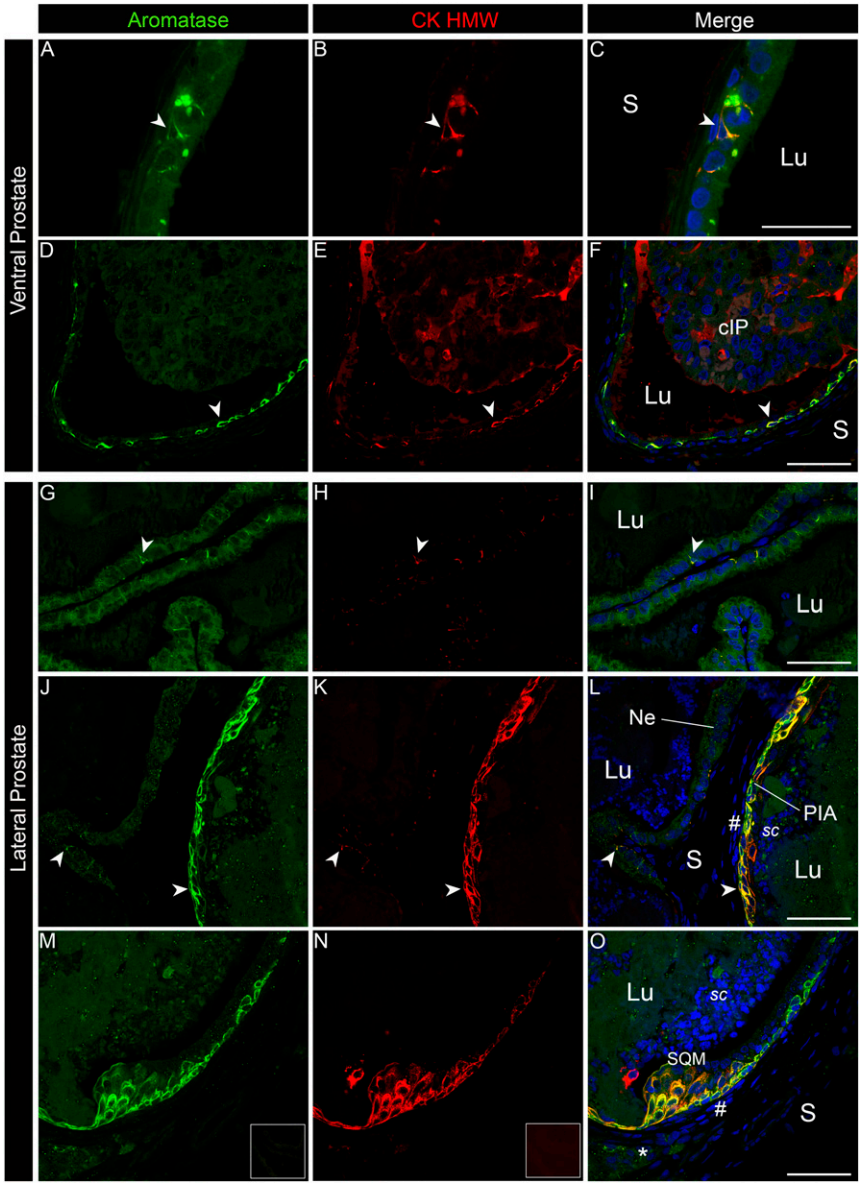

Figure 4. Colocalization of aromatase and the basal cell marker CK HMW in the ventral and lateral prostate. (A–C, G–I) Aromatase and CK HMW were colocalized in sporadic basal cells of the normal epithelium. Increased occurrence of cells colocalizing in areas of histopathological lesions found in aging prostates: (D–F) cIP in the ventral prostate; (J–L) PIA; and (M–O) SQM. Merge: overlay of green, red, and blue (4′,6-diamidino-2-phenylindole) filters; scale bar = 100 μm. Inferior insets are images of negative controls. Arrowheads indicate Arom+basal cells. #, thickening of the stroma; *, inflammatory infiltrate; cIP, cribriform intraepithelial proliferation; Lu, lumen; Ne, normal epithelium; S, stroma; *sc*, sloughed cells into the lumen; SQM, squamous metaplasia.

However, a significant increase in the frequency and distribution of these cells was observed in areas of proliferative and inflammatory changes found in the senile prostate. These cells appeared concentrated in focal areas of PIA, squamous metaplasia, and prostatitis, suggesting a potential link between local areas of estrogen activity and the development of prostate lesions in the aging rat.

The current study provides data that demonstrate the epithelium may, indeed, be a source for the production of estrogen in the aging rat prostate, particularly coming from the basal cells. However, the source of intraprostatic estrogen still remains a matter of debate. Higher density of basal cells in the prostate of estrogenized rodents has already been described, although without reference to aromatase expression (5, 36, 39, 40). Similarly, hyperplasia of basal cells has been found associated with inflammation in the peripheral zone of human prostate (41). Despite the unknown mechanism, there is growing evidence that estrogens may play a role in developing premalignant and malignant lesions in the prostate (3, 5–7, 11, 12, 36, 39). Data from aromatase knockout mice corroborate this, revealing that they do not develop cancer or inflammation in the prostate (4, 12). Overall, these data support the idea that Arom+basal cells may produce an imbalance in the intraorgan hormones, favoring an increase in estrogen action and, ultimately, leading to the local progression of prostatic lesions. It is important to highlight that, as previously shown (30), the aging animals do not present variations in estrogen levels in the plasma or total prostate. The relevance of systemic hormone measurement for determining prostate pathologies has long been criticized. If, indeed, the hypothesis linking estrogen to the onset of prostate disease continues to be supported, data presented here, showing a significant increase in focal aromatase expression without a change in total plasma estrogen levels (30), become clinically relevant because they raise an important question of how to assess more sensitively the potential changes in intraprostatic estrogen levels.

A growing body of evidence shows that aberrant proliferative alterations and inflammation induced by estrogens are mainly mediated by ERα, not ERβ (5, 7, 12). Usually, ERα is barely detectable in prostate, being mainly found in some stromal cells. Hormone-induced neoplasia and metaplasia have been shown to greatly increase the expression of ERα in mouse prostatic epithelium (12, 39). By using tissue recombination obtained

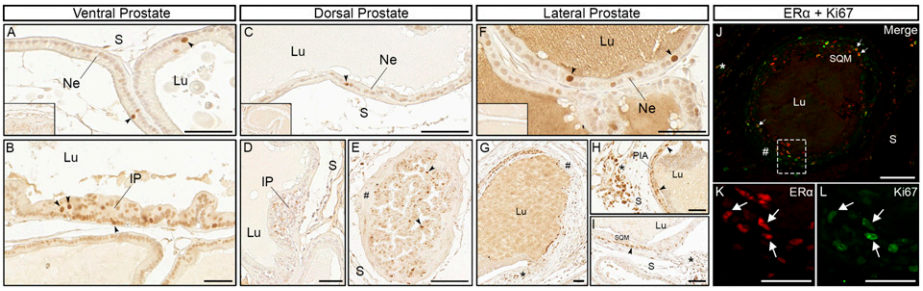

Figure 5. Immunolocalization of ERα in aging rat prostates. (A, C, F) ERα-positive nuclei were found in scarce cells into the normal epithelium of the ventral, dorsal, and lateral prostates, respectively. The ERα-positive nuclei were more frequent in areas of (B, D) IP; (E) hyperplasia; (G, I) metaplasia; and (H) PIA. These positive nuclei were observed in the epithelium associated with thickening of the adjacent stroma (#) and inflammation (*). (J–L) Colocalization of ERα (red) and the proliferation marker Ki67 (green) in areas of squamous metaplasia. Merge: overlay of green and red filters; scale bars = 50 μm; Insets are images of negative controls. Arrowheads indicate positive nuclei; arrows indicate ERα- and Ki67-positive nuclei. IP, intraepithelial proliferation; Lu, lumen; Ne, normal epithelium; S, stroma; SQM = squamous metaplasia.

from transgenic mice overexpressing aromatase, Ellem *et al.* (11) also demonstrated that local aromatase overexpression induces prostate epithelial ERα. Herein, we found increased expression of ERα, which corresponded to the increase in aromatase at focal areas of intraepithelial proliferation as well as inflammation. On the other hand, we previously demonstrated that ERβ expression is greatly reduced in areas of proliferative disorders and premalignant lesions of aging prostates (30). These areas of ERβ reduction were associated with increased cell proliferation, thus providing evidence of an imbalance in tissue homeostasis (37).

It was noteworthy that in the lateral prostate tissue lesions suggestive of inflammatory atrophy of the prostate and squamous metaplasia were also lesions with higher frequency of Arom+basal cells. Squamous metaplasia in the prostate is a well-known response to estrogen treatment (36, 39). Others have also shown that estrogens can lead to an inflammatory predisposition (5, 11, 39, 42). As such, it is known that the aromatase promotor PII is regulated by inflammatory cytokines that are increased in aging prostates (9, 43, 44). These data point to a vicious cycle in which local inflammation produces cytokines that induce aromatase, thus increasing estrogens and further inflammation. Although inflammation was not the focus of this study, we observed mast cells in the inflammatory infiltrate adjacent to epithelial lesions, which corroborates data from the literature that observed increased mast cells in the prostate of adult transgenic mice overexpressing aromatase (11). Considering that inflammation has been implicated in the etiology of prostate cancer, our present data become of greater interest and deserve further investigation.

In conclusion, these findings support the hypothesis that a local increase in aromatase and, consequently, estrogens, associated with ERβ reduction could favor prostate epithelial proliferation and metaplastic changes via an increase in ERα, specifically in association with inflammatory foci. Such local hormonal imbalances would favor the development of pathological changes in the prostate.

Acknowledgments

We thank Dr. Geovanni Cassali for generous donation of the anti-ERα antibody and Dr. Helio Chiarini Garcia for donation of the anti-Ki67 antibody.

Financial Support: This study was supported by the Conselho Nacional de Desenvolvimento Científico e Tecnológico–Brazil (Grant 4739/2013-0 and research fellowship to C.A.O., doctoral fellowship to M.M.-S., master fellowship to G.H.C.-S., and Programa Institucional de Bolsas de Iniciação Científica (PROBIC) scholarship to H.W.-G.); Fundação de Amparo à Pesquisa do Estado de Minas Gerais–Brazil (Grant PPM-00334-14 to C.A.O. and PROBIC scholarship to L.C.S.) and Pró-Reitoria de Pesquisa–Universidade Federal de Minas Gerais.

Correspondence: Cleida A. Oliveira, PhD, Av. Antônio Carlos, 6627 - CEP 31270-901, Belo Horizonte, Minas Gerais, Brazil. E-mail: cleida@icb.ufmg.br.

Disclosure Summary: The authors have nothing to disclose.

References

1. Cooke PS, Nanjappa MK, Ko C, Prins GS, Hess RA. Estrogens in male physiology. *Physiol Rev*. 2017;**97**(3):995–1043.
2. Bosland MC, Ford H, Horton L. Induction at high incidence of ductal prostate adenocarcinomas in NBL/Cr and Sprague-Dawley Hsd:SD rats treated with a combination of testosterone and estradiol-17 beta or diethylstilbestrol. *Carcinogenesis*. 1995;**16**(6):1311–1317.
3. Hu WY, Shi GB, Lam HM, Hu DP, Ho SM, Madueke IC, Kajdacsy-Balla A, Prins GS. Estrogen-initiated transformation of prostate epithelium derived from normal human prostate stem-progenitor cells. *Endocrinology*. 2011;**152**(6):2150–2163.
4. McPherson SJ, Wang H, Jones ME, Pedersen J, Iismaa TP, Wreford N, Simpson ER, Risbridger GP. Elevated androgens and prolactin in aromatase-deficient mice cause enlargement, but not malignancy, of the prostate gland. *Endocrinology*. 2001;**142**(6):2458–2467.
5. Prins GS, Birch L, Habermann H, Chang WY, Tebeau C, Putz O, Bieberich C. Influence of neonatal estrogens on rat prostate development. *Reprod Fertil Dev*. 2001;**13**(4):241–252.

6. Prins GS, Birch L, Tang WY, Ho SM. Developmental estrogen exposures predispose to prostate carcinogenesis with aging. *Reprod Toxicol*. 2007;**23**(3):374–382.
7. Risbridger G, Wang H, Young P, Kurita T, Wang YZ, Lubahn D, Gustafsson JA, Cunha G. Evidence that epithelial and mesenchymal estrogen receptor-alpha mediates effects of estrogen on prostatic epithelium [published correction appears in Dev Biol. 2001;231(1): 289]. *Dev Biol*. 2001;**229**(2):432–442.
8. Siegel R, Ma J, Zou Z, Jemal A. Cancer statistics, 2014. *CA Cancer J Clin*. 2014;**64**(1):9–29.
9. Ellem SJ, Risbridger GP. Aromatase and regulating the estrogen: androgen ratio in the prostate gland. *J Steroid Biochem Mol Biol*. 2010;**118**(4-5):246–251.
10. Simpson ER, Clyne C, Rubin G, Boon WC, Robertson K, Britt K, Speed C, Jones M. Aromatase–a brief overview. *Annu Rev Physiol*. 2002;**64**(1):93–127.
11. Ellem SJ, Wang H, Poutanen M, Risbridger GP. Increased endogenous estrogen synthesis leads to the sequential induction of prostatic inflammation (prostatitis) and prostatic pre-malignancy. *Am J Pathol*. 2009;**175**(3):1187–1199.
12. Ricke WA, McPherson SJ, Bianco JJ, Cunha GR, Wang Y, Risbridger GP. Prostatic hormonal carcinogenesis is mediated by in situ estrogen production and estrogen receptor alpha signaling. *FASEB J*. 2008;**22**(5):1512–1520.
13. Kaburagi Y, Marino MB, Kirdani RY, Greco JP, Karr JP, Sandberg AA. The possibility of aromatization of androgen in human prostate. *J Steroid Biochem*. 1987;**26**(6):739–742.
14. Stone NN, Fair WR, Fishman J. Estrogen formation in human prostatic tissue from patients with and without benign prostatic hyperplasia. *Prostate*. 1986;**9**(4):311–318.
15. Block JL, Block NL, Lokeshwar BL. Inhibition of aromatase activity and growth suppression by 4-methoxy-4-androstene-3,17-dione in an androgen sensitive human prostatic carcinoma cell line. *Cancer Lett*. 1996;**101**(2):143–148.
16. Hiramatsu M, Maehara I, Ozaki M, Harada N, Orikasa S, Sasano H. Aromatase in hyperplasia and carcinoma of the human prostate. *Prostate*. 1997;**31**(2):118–124.
17. Matzkin H, Soloway MS. Immunohistochemical evidence of the existence and localization of aromatase in human prostatic tissues. *Prostate*. 1992;**21**(4):309–314.
18. Takase Y, Lévesque MH, Luu-The V, El-Alfy M, Labrie F, Pelletier G. Expression of enzymes involved in estrogen metabolism in human prostate. *J Histochem Cytochem*. 2006;**54**(8):911–921.
19. Tsugaya M, Habib FK, Chisholm GD, Ross M, Tozawa K, Hayashi Y, Kohri K, Tanaka S. Testosterone metabolism in primary cultures of epithelial cells and stroma from benign prostatic hyperplasia. *Urol Res*. 1996;**24**(5):265–271.
20. Brodie AM, Son C, King DA, Meyer KM, Inkster SE. Lack of evidence for aromatase in human prostatic tissues: effects of 4-hydroxyandrostenedione and other inhibitors on androgen metabolism. *Cancer Res*. 1989;**49**(23):6551–6555.
21. Negri-Cesi P, Poletti A, Colciago A, Magni P, Martini P, Motta M. Presence of 5alpha-reductase isozymes and aromatase in human prostate cancer cells and in benign prostate hyperplastic tissue. *Prostate*. 1998;**34**(4):283–291.
22. Smith T, Chisholm GD, Habib FK. Failure of human benign prostatic hyperplasia to aromatise testosterone. *J Steroid Biochem*. 1982;**17**(1):119–120.
23. Voigt KD, Bartsch W. Intratissular androgens in benign prostatic hyperplasia and prostatic cancer. *J Steroid Biochem*. 1986; **25**(5, 5B)749–757.
24. Ho CK, Nanda J, Chapman KE, Habib FK. Oestrogen and benign prostatic hyperplasia: effects on stromal cell proliferation and local formation from androgen. *J Endocrinol*. 2008;**197**(3):483–491.
25. Pelletier G. Expression of steroidogenic enzymes and sex-steroid receptors in human prostate. *Best Pract Res Clin Endocrinol Metab*. 2008;**22**(2):223–228.
26. Ellem SJ, Schmitt JF, Pedersen JS, Frydenberg M, Risbridger GP. Local aromatase expression in human prostate is altered in malignancy. *J Clin Endocrinol Metab*. 2004;**89**(5):2434–2441.
27. Gianfrilli D, Pierotti S, Pofi R, Leonardo C, Ciccariello M, Barbagallo F. Sex steroid metabolism in benign and malignant intact prostate biopsies: individual profiling of prostate intracrinology. *Biomed Res Int*. 2014;**2014**:464869.
28. Marts SA, Padilla GM, Petrow V. Aromatase activity in microsomes from rat ventral prostate and Dunning R3327H rat prostatic adenocarcinoma. *J Steroid Biochem*. 1987;**26**(1):25–29.
29. Castro B, Sánchez P, Torres JM, Preda O, del Moral RG, Ortega E. Bisphenol A exposure during adulthood alters expression of aromatase and 5α-reductase isozymes in rat prostate. *PLoS One*. 2013; **8**(2):e55905.
30. Morais-Santos M, Nunes AE, Oliveira AG, Moura-Cordeiro JD, Mahecha GA, Avellar MC, Oliveira CA. Changes in estrogen receptor ERβ (ESR2) expression without changes in the estradiol levels in the prostate of aging rats. *PLoS One*. 2015;**10**(7): e0131901.
31. Oliveira AG, Coelho PH, Guedes FD, Mahecha GA, Hess RA, Oliveira CA. 5alpha-Androstane-3beta,17beta-diol (3beta-diol), an estrogenic metabolite of 5alpha-dihydrotestosterone, is a potent modulator of estrogen receptor ERbeta expression in the ventral prostrate of adult rats. *Steroids*. 2007;**72**(14):914–922.
32. Bourguiba S, Genissel C, Lambard S, Bouraïma H, Carreau S. Regulation of aromatase gene expression in Leydig cells and germ cells. *J Steroid Biochem Mol Biol*. 2003;**86**(3-5):335–343.
33. Martins-Santos E, Pimenta CG, Campos PRN, Franco MB, Gomes DA, Mahecha GAB, Oliveira CA. Persistent testicular structural and functional alterations after exposure of adult rats to atrazine. *Reprod Toxicol*. 2017;**73**:201–213.
34. Stocco C. Aromatase expression in the ovary: hormonal and molecular regulation. *Steroids*. 2008;**73**(5):473–487.
35. Shum WW, Da Silva N, McKee M, Smith PJ, Brown D, Breton S. Transepithelial projections from basal cells are luminal sensors in pseudostratified epithelia. *Cell*. 2008;**135**(6):1108–1117.
36. Risbridger GP, Wang H, Frydenberg M, Cunha G. The metaplastic effects of estrogen on mouse prostate epithelium: proliferation of cells with basal cell phenotype. *Endocrinology*. 2001;**142**(6): 2443–2450.
37. Gonzaga ACR, Campolina-Silva GH, Werneck-Gomes H, Moura-Cordeiro JD, Santos LC, Mahecha GAB, Morais-Santos M, Oliveira CA. Profile of cell proliferation and apoptosis activated by the intrinsic and extrinsic pathways in the prostate of aging rats. *Prostate*. 2017;**77**(9):937–948.
38. West NB, Roselli CE, Resko JA, Greene GL, Brenner RM. Estrogen and progestin receptors and aromatase activity in rhesus monkey prostate. *Endocrinology*. 1988;**123**(5):2312–2322.
39. Bianco JJ, Handelsman DJ, Pedersen JS, Risbridger GP. Direct response of the murine prostate gland and seminal vesicles to estradiol. *Endocrinology*. 2002;**143**(12):4922–4933.
40. Putz O, Schwartz CB, Kim S, LeBlanc GA, Cooper RL, Prins GS. Neonatal low- and high-dose exposure to estradiol benzoate in the male rat: I. Effects on the prostate gland. *Biol Reprod*. 2001;**65**(5): 1496–1505.
41. Thorson P, Swanson PE, Vollmer RT, Humphrey PA. Basal cell hyperplasia in the peripheral zone of the prostate. *Mod Pathol*. 2003;**16**(6):598–606.
42. Risbridger GP, Ellem SJ, McPherson SJ. Estrogen action on the prostate gland: a critical mix of endocrine and paracrine signaling. *J Mol Endocrinol*. 2007;**39**(3):183–188.
43. Maggio M, Basaria S, Ceda GP, Ble A, Ling SM, Bandinelli S, Valenti G, Ferrucci L. The relationship between testosterone and molecular markers of inflammation in older men. *J Endocrinol Invest*. 2005; **28**(11, Suppl Proceedings):116–119.
44. Risbridger GP, Bianco JJ, Ellem SJ, McPherson SJ. Oestrogens and prostate cancer. *Endocr Relat Cancer*. 2003;**10**(2):187–191.